IEEE Access
Multidisciplinary ⋮ Rapid Review ⋮ Open Access Journal

Received September 24, 2020, accepted October 22, 2020, date of publication November 24, 2020,
date of current version December 8, 2020.

Digital Object Identifier 10.1109/ACCESS.2020.3040102

Effects of Thermal Relaxation on Temperature Elevation in *Ex Vivo* Tissues During High Intensity Focused Ultrasound

CHENGHAI LI[1], SIYAO CHEN[1], QI WANG[2], HAO LI[1], SHUAI XIAO[1], AND FAQI LI[1]
[1]State Key Laboratory of Ultrasound in Medicine and Engineering, College of Biomedical Engineering, Chongqing Medical University, Chongqing 400016, China
[2]Chongqing Key Laboratory of Biomedical Engineering, Chongqing Medical University, Chongqing 400016, China

Corresponding author: Faqi Li (lifq@cqmu.edu.cn)

This work was supported in part by the National Natural Science Foundation of China under Grant 11574039 and Grant 12004059, in part by the Chongqing Municipal Natural Science Foundation under Grant cstc2020jcyj-msxmX0456, and in part by the Chongqing Special Postdoctoral Science Foundation.

ABSTRACT The introduction of thermal relaxation makes non-Fourier heat transfer more effective than Pennes equation to reflect rapid bio-heat transferring during HIFU, however, the contribution of thermal relaxation in specific tissues needs to be further clarified. In this study, we first measured the thermal relaxation times of porcine muscle and porcine fat. Combining with experimental measurements, the effects of thermal relaxation on temperature elevation in the tissues were investigated by using Pennes equation, thermal wave model of bio-heat transfer (TWMBT) and dual phase-lag (DPL) bio-heat transfer. Results showed that: a) The thermal relaxation times of porcine muscle and porcine fat are experimentally determined as 5.71±0.11 s and 5.02±0.06 s, respectively. b) In the absence of cavitation, DPL bio-heat transfer is more accurate to predict the temperature elevation at the focus and 2 mm from the focus than Pennes equation and TWMBT. Particularly, comparing with the reported of bologna (16 s) used in most of the theoretical analysis, the utilization of the measured thermal relaxation time for a specific tissue in DPL bio-heat transfer is more effective in predicting the temperature elevation during HIFU. c) Acoustic cavitation and nonlinear propagation is easier to happen in fat, under which all bio-heat transfer models are failed to forecast the temperature elevation induced by HIFU. The results demonstrate that different tissues have different thermal relaxation, DPL bio-heat transfer with the measured thermal relaxation times of specific tissues can accurately predict the temperature elevation during HIFU without cavitation.

INDEX TERMS Bio-heat transfer, thermal relaxation, high intensity focused ultrasound.

I. INTRODUCTION

High intensity focused ultrasound(HIFU), as a non-invasive therapeutic technique, has been proven effective and successful in treating malignant and benign solid tumors, including liver cancer, breast cancer, uterine fibroids among others [1]. In the applications of HIFU, an ultrasonic beam was focused at a preselected area causes a local temperature elevation to over 60 °C, leading to irreversible coagulation necrosis in tissues, while energy density outside the target area is usually low, the treatment could be considered safe for neighboring tissues [2]. In order to achieve precision therapy, accurate prediction of temperature distribution is necessary before HIFU.

For a long time, heat transfer in biological tissues is usually predicted with the well-known Pennes equation proposed in 1948 [3], [4], which describes heat conduction in terms of the Fourier series expansion. However, when used to describe temperature distribution in hyperthermia such as HIFU, microwave, and radiofrequency ablation, validity of Pennes equation faces challenge [5]. On the one hand, the theory of Fourier conduction assumes that heat propagate at infinite speeds in media, while the establishment of any thermal equilibrium will take a period of time [6]. On the other hand, the phenomenon of wavelike temperature oscillation is observed during *in vivo* bio-heat transfer [7], while Pennes equation is incapable of explaining. To account for

The associate editor coordinating the review of this manuscript and approving it for publication was Vincent Chen.

that, by introducing Cattaneo-Vernotte(CV) hyperbolic heat transfer into traditional Pennes bio-heat transfer equation, Liu *et al.* [8] proposed the Thermal wave model of bio-heat transfer (TWMBT) to describe unsteady heat transferring. The authors further conducted a preliminary interpretation on the mechanisms of the temperature oscillations in living tissues [8], [9].

TWMBT were then used to study heat transfer in biological tissues during hyperthermia with heating sources of laser [10], [11], microwave [12], radiofrequency [13]. When a multi-layer tissue phantom was irradiated with short pulse laser, Jaunich *et al* compared the temperature response predicted with TWMBT and Pennes equation, found that the former roughly consistent with the experimental results [10]. Ahmadikia *et al.* [11] theoretically analyzed the applicable conditions of different bio-heat transfer models during laser irradiation, concluded that the discrepancy between the results of TWMBT and Pennes model was negligible during laser heating with large albedo, while non-Fourier effect should be considered during laser heating with low albedo. Ozen *et al* used microwave as heating source, and found that the increasing rate of tissue temperature predicted with TWMBT was lower than that with Pennes equation, while the two models tended to give consistent results as the time went by [12]. Through a voltage-calibration method, Zhang *et al* investigated the feasibility of TWMBT in the radiofrequency ablation (RFA) simulation, the results suggested that the prediction of TWMBT was 0.55 °C more accurate than Pennes equation, declared that TWMBT could be used as an alternative in the simulation of long-duration high intensity RFA [13]. In recent years, TWMBT also has been employed to study bio-heat transfer during HIFU [14]–[17]. Liu *et al.* [14] and Gupta and Srivastava [16] used TWMBT to estimate the temperature elevation induced by HIFU in biological tissues. The simulated results showed that, since exist of thermal relaxation, TWMBT leaded to lower temperature estimation than that based on Pennes equation during the same exposure situation.

On the other hand, in order to study rapid heat transfer between internal elements of heterogeneous materials, Tzou *et al* obtained a dual phase-lag (DPL) model through introducing phase lags τ_q and τ_T arising from ''thermal inertia'' and ''microstructural interaction'', respectively [18], [19]. Then combined the theory of DPL and transfer equation, the author presented the lagging behavior in biological systems, such as drug delivery in tumors and heat exchanging between tissue and blood [20]. In another research, DPL bio-heat transfer was also applied to investigate thermal damage induced by laser irradiation. It was shown that DPL model provided significantly different prediction for temperature and thermal damage from Pennes model, DPL equation reduced to the classical Pennes equation when phase lag times were zero [21]. Liu *et al* analyzed the thermal response of living tissue with blood perfusion and metabolic heat generation during laser irradiation [22] and magnetic hyperthermia [23], the results showed that the total effect of τ_q and τ_T on the bio-heat transfer relied on ratio of τ_q and τ_T, DPL model could be reduced to Fourier bio-heat transfer for $\tau_q = \tau_T$. At the same time, Xu *et al.* [24] and Lin *et al.* [25] presented some valuable results on the use of DPL bio-heat model in skin biothermomechanics and human tooth. The above research reveals that DPL bio-heat transfer can be an effective tool to investigate inhomogeneous-anisotropic material such as HIFU-exposing biological tissue. In our previous research, we explored the possibility of using DPL model in HIFU hyperthermia to study HIFU-induced temperature elevation in heterogeneous liver tissues [26]. However, the research on thermal relaxation and it's effect on bio-heat transfer for common human tissues is still absent.

In order to achieve accurate prediction of heat behavior in biological tissues, some crucial and effective parameters will be used, e.g., the thermal conductivity, the specific heat capacity, and the thermal relaxation time, which is defined as the characteristic time needed for accumulating the thermal energy required for propagative transfer to the nearest element within the nonhomogeneous inner structures [8]. The introduction of thermal relaxation time make DPL bio-heat transfer different from classical Pennes equation. However, the use of thermal relaxation in specific tissues is still unclear. Generally, the thermal relaxation time is a constant for a given medium [6], for homogeneous media it usually lies in the range 10^{-8}-10^{-14}s [27]. For biological tissues, theoretical estimate of thermal relaxation to be 1-100 s at room temperature [28]. Mitra *et al.* [29] reported a thermal relaxation time of processed meat (bologna) was ∼16s, while the result from Roetzel *et al.* [30] was ∼1.77 s. For most theoretical analysis, the used thermal relaxation time usually come from the experimental results of processed meat (bologna), which was measured by Mitra in 1995 [29]. In fact, most of the human soft tissues, e.g., liver, kidney, heart, and muscle have similar thermal properties, however, some tissue such as fat whose thermal conductivity and specific heat capacity are smaller than the formers [31]. On account of the physical reality that thermal relaxation time is based on thermal properties, it is necessary to take into account the specific thermal relaxation time for a tissue in theoretical prediction.

In this paper, porcine muscle and porcine fat are chosen for their proximity with the human's, whose thermal relaxation times are determined by experimentally measured. Followed that, the effects of thermal relaxation on temperature elevation in the tissues were investigated by combining experimental measurement and theoretical simulation of Pennes equation, TWMBT and DPL bio-heat transfer. The effect of HIFU-induced cavitation on bio-heat transfer will be discussed as well.

II. MATERIALS AND METHODS

A. THEORETICAL MODELS AND SIMULATION

Nonlinear propagation of HIFU in biological tissue can be described with the Khokhlov-Zabolotskaya-Kuznetsov (KZK) equation [32], [33], which incorporates diffraction,

attenuation and nonlinearity, whose form in cylindrical coordinate is written as follows

$$\frac{\partial^2 p}{\partial z \partial t'} = \frac{c_0}{2}\Delta_\perp p + \frac{b}{2\rho_0 c_0^3}\frac{\partial^3 p}{\partial t'^3} + \frac{\beta}{2\rho_0 c_0^3}\frac{\partial^2 p^2}{\partial t'^2} \tag{1}$$

where $p(z, r, t)$ is the acoustic pressure; $t' = t - z/c_0$ is the time delay with t, z, and c_0 being the time, the axial coordinate and the sound velocity, respectively; ρ_0 is the density of the medium; b is the absorption parameter of the medium, β is the nonlinear coefficient. $\Delta_\perp$ is the two-dimensional Laplacian operator; For an axisymmetric FU beam, the acoustic pressure field is independent of the polar angle. Therefore, in cylindrical coordinate system $\Delta_\perp = \partial^2/\partial r^2 + (\partial/\partial r)/r$, with r being the radial coordinate.

Numerical solutions of (1) can be achieved with finite difference in frequency domain (FDFD) method. Using Fourier series, the acoustic pressure p is expanded as

$$p(z, r, t) = \sum_{n=-\infty}^{+\infty} C_n(z, r)\, e^{jn\omega_0 \tau} \tag{2}$$

in which ω_0 is the fundamental angular frequency of p, j is the imaginary unit and C_n is the amplitude of the nth harmonic component.

When HIFU propagate through a tissue, part of its energy is absorbed and convert into heat. For *in vitro* tissue, blood perfusion and metabolism are ignored, the bio-heat transfer equation is given as [6]

$$\frac{\partial T(z, r, t)}{\partial t} = -\frac{\nabla \cdot \vec{q}(z, r, t)}{\rho_0 C_t} + \frac{Q(z, r)}{\rho_0 C_t} \tag{3}$$

where $T(z, r, t)$ and C_t are the tissue temperature and specific heat capacity, ∇ is the Hamilton operator. $\vec{q}(z, r, t)$ is the heat flux vector, representing heat flow per unit time, per unit area in the direction of temperature increase. $Q(z, r)$ is the source term, represents the acoustic energy absorbed by the tissue of unit volume, being expressed as

$$Q(z, r) = \frac{1}{\rho_0 c_0}\sum_{n=1}^{N} 4\alpha_0 n^\mu |C_n(z, r)|^2 \tag{4}$$

Here N is the highest harmonic order ($N = 50$ in the study), $\alpha_0 = \omega_0^\mu b/(2\rho_0 c_0^3)$ is the attenuation coefficient of the tissue, μ is the intensity index. Based on the Fourier theory of heat analysis, $\vec{q}(z, r, t)$ can be given as

$$\vec{q}(z, r, t) = -\kappa \nabla T(z, r, t) \tag{5}$$

i.e., the spatial gradient of temperature, in which κ is the heat conductivity. Substituting (5) into (3) gives the Pennes equation [3]

$$\frac{\partial T(z, r, t)}{\partial t} = \frac{\kappa}{\rho_0 C_t}\nabla^2 T(z, r, t) + \frac{Q(z, r)}{\rho_0 C_t} \tag{6}$$

By recognizing the propagation speed of heat to be finite, thermal relaxation time τ_q and τ_T are then introduced, and from (5) one can obtain dual phase-lag (DPL) [18] model written as

$$\vec{q}(z, r, t + \tau_q) = -\kappa \nabla T(z, r, t + \tau_T) \tag{7}$$

In this model, τ_q is the time lag between heat flux and the associated heat conduction through a medium, representing the period arising from thermal inertia; τ_T is the time lag responsible for establishing temperature gradient through a medium with microstructure [19], describing thermal interactions between different sub-structures. Here, the thermal relaxation time $\tau_q = \alpha/\upsilon^2$, in which $\alpha = \kappa/\rho_0 C_t$ is the thermal diffusivity of the medium. The thermal wave speed $\upsilon = x_m/t_m$, with x_m being the distance between the detection point and the heat source, and t_m being the corresponding time required for heat to propagate. DPL model will be reduced to TWMBT for $\tau_q \neq 0$, $\tau_T = 0$, and Pennes equation for $\tau_q = \tau_T = 0$.

Different expansion of heat flow vector $\vec{q}(z, r, t + \tau_q)$ and corresponding temperature $T(z, r, t + \tau_T)$ can lead to different forms of DPL models, here, $\vec{q}(z, r, t + \tau_q)$ and $T(z, r, t + \tau_T)$ are expanded with first order Taylor series, and (7) is expressed as

$$\vec{q}(z, r, t) + \tau_q \frac{\partial \vec{q}(z, r, t)}{\partial t} = -\kappa\left[\nabla T(z, r, t) + \tau_t \frac{\partial \nabla T(z, r, t)}{\partial t}\right] \tag{8}$$

Substituting (8) into (3) give the DPL bio-heat transfer model

$$\begin{aligned}\tau_q \rho_0 C_t \frac{\partial^2 T(z, r, t)}{\partial t^2} &= \kappa \nabla^2 T(z, r, t) + \tau_t \kappa \nabla^2 \frac{\partial \nabla T(z, r, t)}{\partial t} \\ &\quad - \rho_0 C_t \frac{\partial \nabla T(z, r, t)}{\partial t} + \left(Q + \tau_q \frac{\partial \vec{q}(z, r, t)}{\partial t}\right)\end{aligned} \tag{9}$$

The acoustic pressure field could be obtained by a set of coupled differential equations derived from (1) and (2), and calculated numerically using the method of fractional steps with an operator splitting procedure.[22,23] Numerical solutions of (6) and (9) were obtained by applying a regular finite-difference method, as per the procedure mentioned in a previous study.[22] The ultrasound field and temperature elevation were coupled through (4). The model configuration is consistent with that the experiments, which is illustrated in Fig.1. A single-element focused piezoelectric transducer (0.94-MHz central frequency, 16.0-cm focal length, 22.0-cm aperture diameter) immersed in degassed water was used as the heating source. With the transducer surface located at the axial position $z = 0$, the sample surface was at $z = 14$ cm, i.e., the focal area of the transducer was inside the sample. In the finite difference simulations, steps in the spatial and temporal domains were chosen as $\Delta r = 0.05$ mm, $\Delta z = 0.05$ mm, and $\Delta t = 0.01$ s. The adopted thermal and acoustic parameters of the samples are listed in TABLE 1 [31], [34].

TABLE 1. Parameters of water, porcine muscle and porcine fat.

medium	ρ_0 (kg/m^3)	c_0 (m/s)	β	α_0 (Np/m)	κ (W/m/°C)	C_t (W·s/m^3/°C)
Water	1000	1490	3.5	0.025	0.6	4200
Porcine muscle	1060	1550	7.5	15.0	0.51	3140
Porcine fat	971	1430	10.28	7.8	0.185	2700

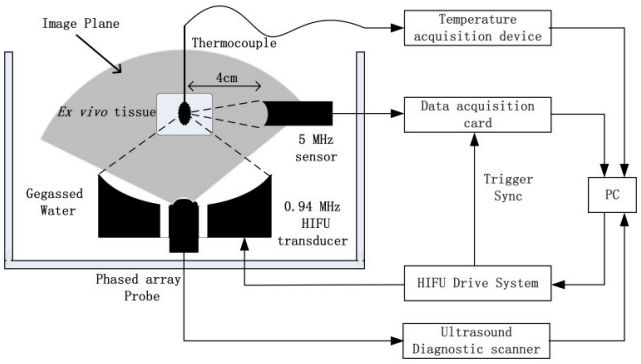

FIGURE 1. Schematic of the experimental setup.

B. EXPERIMENTAL METHODS

Porcine muscle and porcine fat were collected from a slaughterhouse and remained in 0.9% saline at 26 °C, i.e., ambient temperature in the experiment. Then the tissue was cut into cuboid (dimension 80 mm×80 mm×60 mm) and put in a PMMA sample holder (internal dimension 80 mm×80 mm×60 mm). On the front and back sides of holder (perpendicular to the sound axis), two circular acoustic windows were opened, whose diameters were 40 mm. Ultrasonic emission and treatment monitoring was achieved *via* a CFDA and CE-marked extracorporeal High-intensity Focused Ultrasound Tumor Therapeutic device, certified for oncological treatment (Model-JC200 Focused Ultrasound Tumor Therapeutic System, Chongqing Haifu Medical Technology Co., Ltd., Chongqing, China), which contains the waveform generator, RF intensity amplifier, HIFU transducer, water treatment unit, and ultrasound-based monitoring unit, *etc*. HIFU with ultrasonic intensity 727.2 W/cm^2 was used to expose tissues for 20 s. The intensity (free-field spatial-peak) was 727.2 ±11.2 W/cm^2 (n=6), calibrated by a radiation force method [35], [36]. All experiments were performed in a degassed-water bath, gas content were 2.98±0.47 mg/L and 3.05±0.32 mg/L before and after the experiments, determined by a dissolved oxygen meter (550A, YSI, Ohio, USA). After exposure, specimens were immediately sliced into samples sized 20 mm × 40 mm × 5 mm and stained with 2% concentration triphenyl tetrazolium chloride (TTC) solution [37].

The detection system of cavitation and temperature shown as the schematic in Fig. 1. A thermocouple of 0.25-mm diameter (TJ72-CASS-010G-4, Omega, Stamford, CT, USA) was connected to a data acquisition module (9214, National Instruments, Austin, TX, USA) to detect the temperature elevation of HIFU focus and 2 mm from the focus. As described in our previous work [26], the use of thermocouple with the diameter considerably less than the wavelength of ultrasound (about 1.6 mm in this work) will reduce viscous heating artifact of thermocouple. Passive cavitation detection (PCD) and B-mode ultrasound were utilized to monitor acoustic cavitation during HIFU. The PCD system comprised a 5 MHz focused detectors(V309-SU, Olympus NDT Inc, Waltham, MA, USA)and linked to a working platform integrated with a high-speed data acquisition card (PXie-5122, National Instruments, Austin, USA) through a waterproof data line. One diagnostic scanner (Mylab 30cv, Esaote, Genova, Italy) with a phased array probe PA230E (center frequency 3.5 MHz) used for B-mode ultrasound imaging. Equipment synchronization were achieved with the Labview Interface (National Instruments, Austin, TX, USA) on a PC platform. Experiment was repeated 5 times to obtain the statistical results of temperature elevation. The thermal relaxation time τ_q of porcine muscle and porcine fat was determined through heat conductivity κ, specific heat C_t, density ρ_0, and thermal wave velocity υ of the medium. To be specific, bottom of the samples were in contact with heat source (39 °C water bath) at $r = r_0$. The penetration time(t_m) required for heat flow from $r_1 = r_0+$ 2 mm to $r_2 = r_1+4$ mm, and from r_2 to $r_3 = r_2+4$ mm was detected, respectively. By taking $x_m = r_2 - r_1 = r_3 - r_2 =$ 4 mm, t_m for $x_m = 4$ mm was determined through single-tailed Student's t-test by accepting $p < 0.05$ as significance, then υ was calculated as $\upsilon = x_m/t_m$. Each experiment was repeated 3 times, and the heat wave velocity(υ) and thermal relaxation time(τ_q) were determined. In all the experiments, adiabatic foil was used to cover the inner wall of the holder to prevent heat radiation. More detailed measuring methods referred to those in our previous work [26].

III. RESULTS

A. THERMAL RELAXATION TIME

Fig. 2 shows typical results of measured temperature responses at r_1, r_2, and r_3 for porcine muscle and fat.

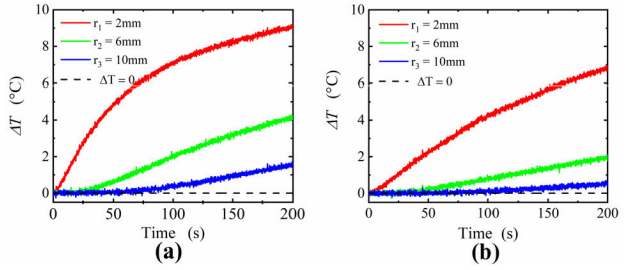

FIGURE 2. Temperature responses measured at the axial locations r_1, r_2, and r_3 for (a) Porcine muscle; (b) Porcine fat. The bottom of the samples were in contact with heat source (39 °C water bath) at r = r_0. The thermocouple is placed at $r_1 = r_0 + 2$ mm, $r_2 = r_1 + 4$ mm and $r_3 = r_2 + 4$ mm to obtain the temperature response.

TABLE 2. Penetration time and relaxation time in Porcine muscle and Porcine fat.

Medium	t_m(s)	τ_q(s)
Porcine muscle	24.42±3.37	5.71±0.11
Porcine fat	34.45±3.82	5.02±0.06

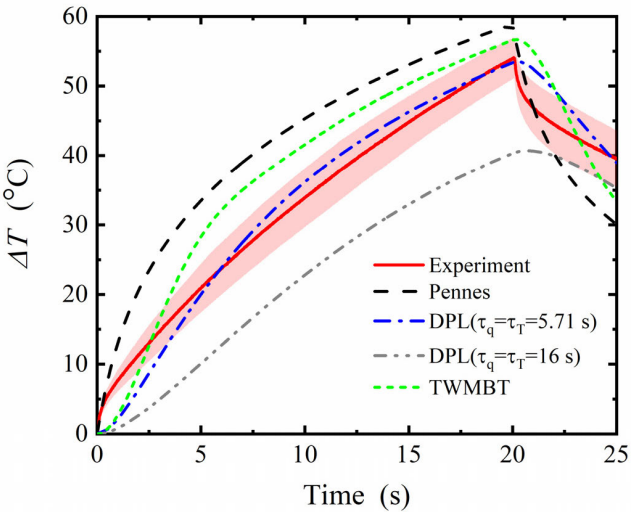

FIGURE 3. Time-dependent temperature elevation at the HIFU focus (z = 160 mm) in porcine muscle, with ultrasonic intensity 727.2 W/cm^2 exposing for 20 s. The red solid lines and pink areas represent the measured averaged results and standard error, respectively, over five repeated experiments.

It is shown that heat conduction in muscle is faster than that in fat. Based on the temperature responses, through single-tailed Student's t-test, the thermal penetration time (t_m) for x_m =4 mm was determined as 24.42±3.37 s and 34.45±3.82 s respectively. According to above description of τ_q, the thermal relaxation time of porcine muscle and porcine fat were calculated as 5.71±0.11 s and 5.02±0.06 s, respectively. Though the same measuring method was employed, it is suggested that the thermal relaxation time of porcine muscle and porcine fat obtained here have big difference from the results of bologna in existing studies [28], [29], but are still reasonable [30].

B. HIFU-INDUCED TEMPERATURE ELEVATION

Fig.3 shows the time-dependent temperature elevation at the focus when porcine muscle was exposed by HIFU with intensity 727.2 W/cm^2 for 20 s. In the beginning of exposure, temperature at HIFU focus increases rapidly since sound energy is absorbed by tissue and convert into heat energy. After that, the temperature increases less rapidly due to the contribution of thermal conduction while source energy remains constant. Except for the initial stage of heating, where the predicted results are slightly low the measured. It is found that the temperature elevation predicted by DPL bio-heat transfer (τ = 5.71 s) lies within the range of the measured during HIFU. After HIFU heating, the temperature gradually decreases with cooling time increases, the rate of the experimental temperature reduction is consistent with the predicted results of DPL bio-heat transfer with the measured thermal relaxation time. However, the theoretical predictions of Pennes equation, TWMBT and DPL bio-heat transfer (τ = 16 s, referred to the thermal relaxation time of bologna [29]) are failed to estimate the temperature variation during heating and cooling. The theoretically predicted temperature of Pennes equation is always higher than the measured, the gap reach a maximum of 12.9 °C at 5.9 s. Though being capable of reducing the rate of temperature rise in the initial stage of heating, the predicted by TWMBT is still higher than the measured. When the thermal relaxation time of bologna (τ = 16 s) [29] was used in DPL bio-heat transfer, the predicted temperature elevation shows a large deviation, the gap reach a maximum of 13.7 °C compared with the measured.

When porcine muscle was exposed by HIFU with intensity of 727.2 W/cm^2 for 20 s, we also investigate the time-dependent temperature elevation at 2 mm from the focus in the axial direction as Fig.4. In addition to the tendency of temperature elevation is consistent with Fig.3, a novel phenomenon is presented. According to the zoomed-in view, the maximum temperature elevation predicted by Pennes equation is 46.14 °C at t = 20 s, when exposure terminate. However, the measured maximum temperature variation is 44.23±2.33 °C at t = 20.1 s (>20 s), and the maximum temperature elevation predicted by DPL bio-heat transfer is 42.52 °C at t = 20.1 s. Although the heating has braked, it is observed that the temperature will continue to increase after exposure, which can be accurately predicted by DPL bio-heat transfer while Pennes bio-heat transfer is failed.

Due to the difference between muscle and fat in acoustic and thermal properties, the same research as porcine muscle was performed in porcine fat. It is observed in Fig.5 that the temperature rises at a higher rate as soon as the exposure starts, the measured maximum temperature elevation is 58.33±10.75 °C when exposure time is ∼5 s. After that, though the exposure time continues to increase, temperature

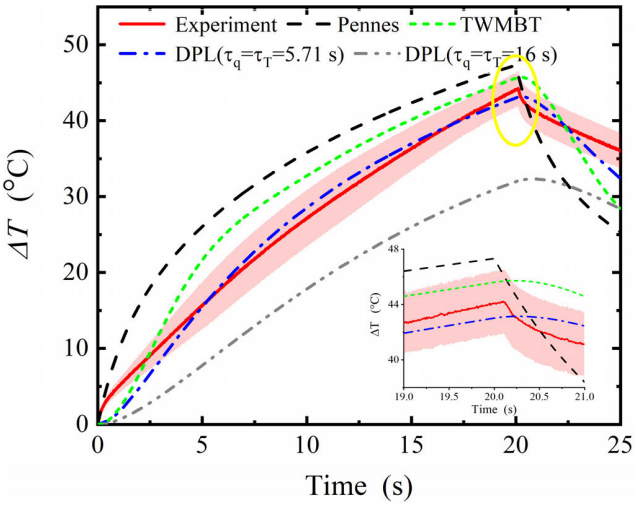

FIGURE 4. Time-dependent temperature elevation at $z = 158$ mm (2 mm from the focal point) in porcine muscle, with ultrasonic intensity 727.2 W/cm^2 exposing for 20 s. The red solid lines and pink areas represent the measured averaged results and standard error, respectively, over five repeated experiments. Zoomed-in view shows more details in 19 s to 21 s.

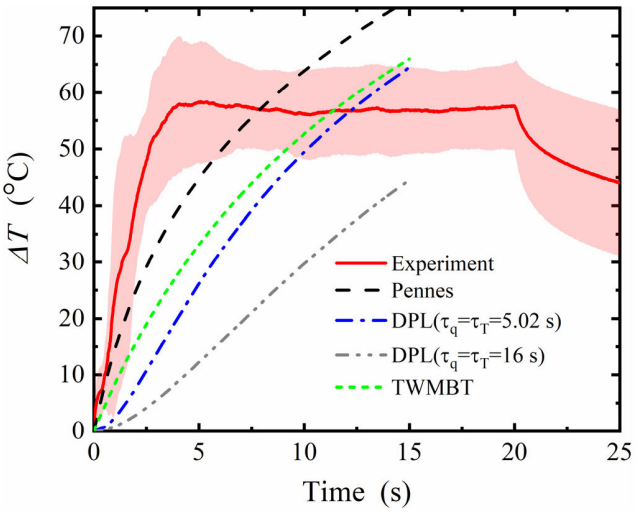

FIGURE 5. Time-dependent temperature elevation at the HIFU focal point ($z = 160$ mm) in porcine fat, with ultrasonic intensity 727.2 W/cm^2 exposing for 20 s. The red solid lines and pink areas represent the measured averaged results and standard error, respectively, over 5 repeated experiments.

elevation induced by HIFU remains constant until the end of exposure (t = 20 s). A large deviation occur between the simulated temperature response and the measured, the prediction of all theoretical modes face challenge, the reasons will be discussed further below.

C. HIFU-INDUCED CAVITATION AND LESION

Exposed by the same HIFU with ultrasonic intensity 727.2 W/cm^2 for 20 s, we investigate the effect of cavitation on bio-heat transfer by experimentally detecting the acoustic emissions and B-scan echogenicity arising from the focus in porcine muscle and fat. It reveals the mechanism of differences in temperature response for different tissues under

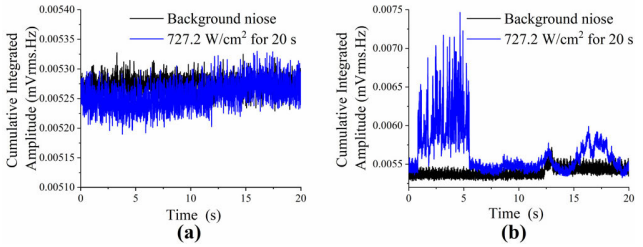

FIGURE 6. Broadband acoustic emission of 3-7 MHz in (a) porcine muscle and (b) porcine fat exposed by HIFU with ultrasonic intensity 727.2 W/cm^2 for 20 s.

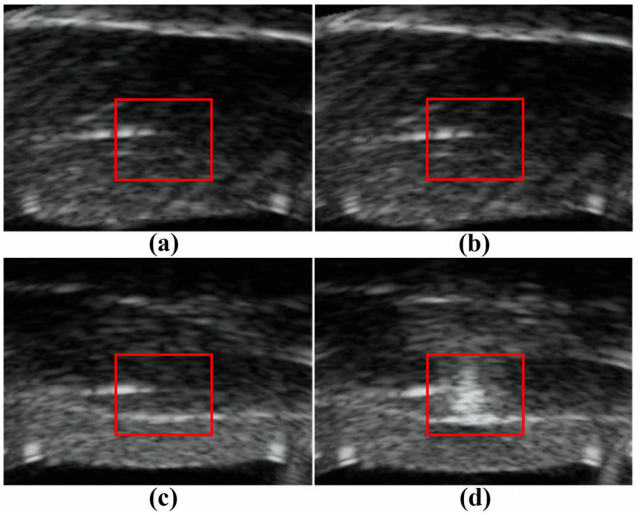

FIGURE 7. B-scan echogenicity on the focal plane before(left) and after(right) HIFU in (a, b) porcine muscle and (c, d) porcine fat exposed by HIFU with ultrasonic intensity 727.2 W/cm^2 for 20 s. The direction of sound propagation is from bottom to top.

the same exposing condition, and illuminates the reason that all theoretical models is failed to predict the temperature elevation in fat during HIFU showing in Fig.5. According to Fig.6(a) for porcine muscle, the amplitude of broadband acoustic emissions of 3-7MHz is at the level of background noise, explain that there is no cavitation occurring during HIFU. This is also certified by B-scan echogenicity in Fig.7(a), no hyperechoic region appears on the focal plane compared with original B-scan image of tissue. Fig.6(b) and Fig.7(b) show completely different results in porcine fat, the amplitude of 3-7MHz acoustic emission is higher than the background noise immediately after the start of exposure, then drop to background noise when the exposure time is ∼5 s and keep floating until the end of exposure. From the contrast result of B-scan echogenicity, a hyperechoic region appears on the focal plane after HIFU. The acoustic emissions and B-scan echogenicity explain that HIFU-induced cavitation occurs in porcine fat during HIFU.

After HIFU, the largest cross-section for maximum lesion of the tissues was obtained along the focal plane as shown in Fig.8. Exposed by the same HIFU exposure condition, the geometry of the lesions in porcine muscle and porcine fat are rice-shape with average area of 44.04±7.63 mm^2

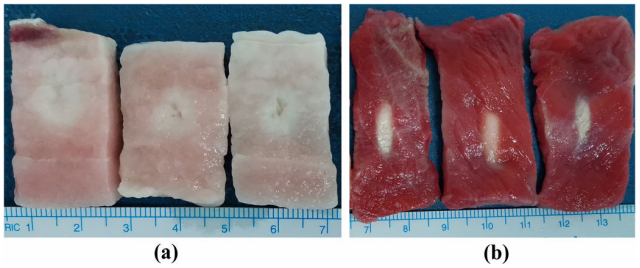

FIGURE 8. The lesions induced by HIFU with ultrasonic intensity 727.2 W/cm^2 for 20 s in (a) porcine fat and (b) porcine muscle. The differences are statistically significant ($p < 0.05$).

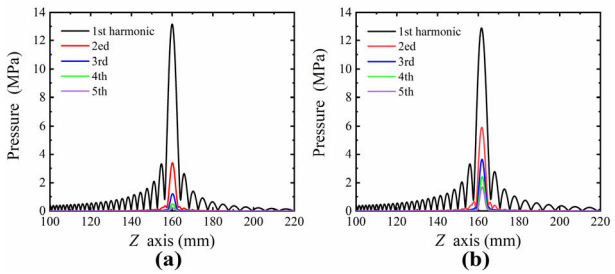

FIGURE 9. The amplitude of first five harmonics in (a) porcine muscle and (b) porcine fat exposed by HIFU with ultrasonic intensity 727.2 W/cm^2 for 20 s.

and droplet-shape with average area of 95.00±17.02 mm^2, respectively. Besides cavitation, we also investigate the nonlinear propagation in tissues exposed by the same HIFU with ultrasonic intensity 727.2 W/cm^2, the amplitude of first five harmonics was shown in Fig.9. Combining with the acoustic cavitation and nonlinear propagation in tissues, it is analyzed and found that the intensity of acoustic cavitation (Fig.6 and Fig.7) and amplitude of the harmonics (Fig.9) in porcine fat are higher than those in porcine muscle. This result reveals that acoustic cavitation and nonlinear propagation are easier to happen in fat, which gives rise to the higher rate of temperature rising(Fig.5) and larger lesion(Fig.8(a)) comparing with muscle(Fig.3 and Fig.8(b)).

IV. DISCUSSION

Heat transfer in biological tissues take places in cells, fluids and soft tissues, have a great difference with homogeneous medium. It makes the Fourier bio-heat transfer, i.e., Pennes equation failed to describe the temperature elevation during hyperthermia and thermal ablation [8], [11], [14], [23]. In this study, the above conclusion is confirmed. Besides, we also find that the theoretical temperature elevation predicted by Pennes equation is always higher than the range of experimental result during HIFU (Fig.3-5). In order to overcome the shortcoming, non-Fourier bio-heat transfer models such as TWMBT [8] and DPL [20] were proposed to describe the heat transfer in biological tissue by introducing thermal relaxation time. Especially, DPL bio-heat transfer provides a more accurate theory than TWMBT to analyze heat transfer in tissues. The reason is that the thermal relaxation arising from both ''thermal inertia'' and ''microstructural interaction'' is taken into account. In this study, similar conclusions are obtained with the previous work [22], [23], [26], we also present a more persuasive evidence to determine the validity of DPL model. When HIFU heating stop at duration time $t = 20$ s, the temperature rise at HIFU focus terminate immediately as Fig.3. However, the temperature at a position 2 mm far from the focal point on the axis continues to rise until $t = 20.1$ s in Fig.4, and is longer than the exposure duration 20 s. The phenomenon was accurately predicted by DPL bio-heat transfer while Pennes bio-heat transfer was failed to predict. This results demonstrate that, the establishment of thermal equilibrium in tissue with finite heat wave velocity need a certain period of time. Sampling period of 10 ms was used to acquire the temperature response induced by HIFU. In the later experimental research, a higher sampling rate will be used to obtain more information about bio-heat transfer.

In addition, our work also suggest the importance of utilization in effective thermal parameters to achieve accurate prediction of heat behavior in biological tissues. For most studies, thermal relaxation time used in bio-heat transfer analysis usually come from the experimental results of processed meat (bologna), which was measured by Mitra in 1995 [29]. Nevertheless, as showed in this study, the thermal relaxation time of porcine muscle and porcine fat are 5.71±0.11 s and 5.02±0.06 s, respectively. Though same measuring method was employed, the result of processed meat (bologna) was ∼16 s measured by Mitra *et al.* [29]. The results declare that different tissues have different thermal relaxation time. In fact, according to the above description of thermal relaxation time, $\tau_q = \kappa/\rho_0 C_t \upsilon^2$, which relies on the heat conductivity, the density and the specific heat capacity of a medium. It's reasonable that the medium with different thermal parameters have different thermal relaxation times. Comparative study in bio-heat transfer was performed by using the thermal relaxation time from measured in this paper and the result of 16 s, respectively. It is found in Fig.3 and Fig.4 that, the temperature elevation with $\tau = 5.71$ s lie within the range of the measured, however, a large deviation exist when the thermal relaxation time of bologna ($\tau = 16$ s) [29] was used. Therefore, the thermal relaxation time of processed meat (bologna) was applied directly to describe bio-heat transfer in other tissues, e.g., muscle and fat, the reasonability should be reconsidered.

Though exciting results were achieved in this work, some vital researches on bio-heat transfer during HIFU should be lucubrated. Firstly, since absence of theory to quantize the thermal relaxation time τ_T of tissues, so $\tau_q = \tau_T$ was used in this paper. However, the choice of τ_T will affect the theoretical results, which has been confirmed by the previous works [22], [23], [26]. This simplification may be the direct reason leading to the deviation between the predicted temperature elevation of DPL model and the measured ones in the initial stage of heating. Secondly, all bio-heat transfer models are yet failed to estimate the temperature elevation in porcine fat heating by HIFU as showed in Fig.5. Combined with HIFU-induced cavitation to analysis, we demonstrate

that cavitation occurs immediately in the initial stage of HIFU in porcine fat, while no cavitation occurs during porcine muscle exposed by HIFU. Therefore, we conclude that it is HIFU-induced cavitation give rise to the deviation between theoretical prediction and experimental measurement. In fact, broadband acoustic emission was observed when porcine fat exposed by HIFU in Fig.6, which represents the occurrence of inertial cavitation [38]. During inertial cavitation, local extremely high temperature will be induced due to collapse of cavitation bubble [39], cavitation will do contribution to enhancing tissue thermal deposition of ultrasound and showed as higher temperature elevation [2], which is difficult to describe in the heat transfer. On the other hand, Liu *et al* observed that the collapse of the cavitation bubble has greater impact on heat transfer while the mechanism is uncertain [40], the generation of cavitation bubble will make heat transfer in tissue more complicated and difficult to predict. In the next study, our work will pay more attention to the effect of HIFU-induced bubble on bio-heat transfer. Another vital factor influence bio-heat transfer during HIFU is blood perfusion, which was ignored in *ex vivo* tissues, exist of blood perfusion takes away heat from the target region and reduces thermal deposition in *in vivo* tissues. It will be another vital research to make sure the effect of blood perfusion on thermal relaxation and temperature elevation during HIFU.

V. CONCLUSION

In order to illuminate the effects of thermal relaxation on bio-heat transfer and achieve theoretical prediction of temperature elevation in biological tissues during HIFU, we measured the thermal relaxation times of porcine muscle and porcine fat. On this basis, combined with measured temperature response, comparative study among the theoretical simulation of Pennes equation, TWMBT and DPL bio-heat transfer in porcine muscle and porcine fat were conducted. Some important conclusions can be determined: (1) The thermal relaxation time of porcine muscle and porcine fat are experimentally determined as 5.71 ± 0.11 s and 5.02 ± 0.06 s, respectively, explain that different tissues have different thermal relaxation. (2) In the absence of cavitation, DPL bio-heat transfer, introducing phase lags τ_q and τ_T arising from ''thermal inertia'' and ''microstructural interaction'', provides more accurate prediction of temperature response during HIFU than Pennes and TWMBT, only taking into account the phase lags τ_q arising from ''thermal inertia''. (3) For simulation of DPL bio-heat transfer in a particular tissue, the result with the measured thermal relaxation time is more accurate at the focus and 2mm from the focus than that with thermal relaxation time of bologna (16 s, used in most of the theoretical analysis). (4) Under the same HIFU, acoustic cavitation and nonlinear propagation is more likely to happen in fat, which give rise to the higher rate of temperature rising and larger lesion than that in muscle. Under cavitation, all bio-heat transfer models are failed to forecast the temperature elevation induced by HIFU. The results presented herein may provide an important reference point for providing accuracy prediction of temperature elevation during HIFU and other thermal ablations.

REFERENCES

[1] K. F. Chu and D. E. Dupuy, ''Thermal ablation of tumours: Biological mechanisms and advances in therapy,'' *Nature Rev. Cancer*, vol. 14, no. 3, pp. 199–208, Mar. 2014.
[2] G. ter Haar and C. Coussios, ''High intensity focused ultrasound: Physical principles and devices,'' *Int. J. Hyperthermia*, vol. 23, no. 2, pp. 89–104, Jan. 2007.
[3] H. H. Pennes, ''Analysis of tissue and arterial blood temperatures in the resting human forearm,'' *J. Appl. Physiol.*, vol. 1, no. 2, pp. 93–122, Aug. 1948.
[4] L. Sebeke, D. A. Deenen, E. Maljaars, E. Heijman, B. de Jager, W. P. M. H. Heemels, and H. Grull, ''Model predictive control for MR-HIFU-mediated, uniform hyperthermia,'' *Int. J. Hyperthermia*, vol. 36, no. 1, pp. 1040–1050, Jan. 2019.
[5] F. Xu, T. Wen, T. Lu, and K. Seffen, ''Skin biothermomechanics for medical treatments,'' *J. Mech. Behav. Biomed. Mater.*, vol. 1, no. 2, pp. 172–187, Apr. 2008.
[6] F. Xu, T. J. Lu, K. A. Seffen, and E. Y. K. Ng, ''Mathematical modeling of skin bioheat transfer,'' *Appl. Mech. Rev.*, vol. 62, no. 5, Sep. 2009, Art. no. 050801.
[7] R. B. Roemer, J. R. Oleson, and T. C. Cetas, ''Oscillatory temperature response to constant power applied to canine muscle,'' *Amer. J. Physiol.-Regulatory, Integrative Comparative Physiol.*, vol. 249, no. 2, pp. R153–R158, Aug. 1985.
[8] J. Liu, X. Chen, and L. X. Xu, ''New thermal wave aspects on burn evaluation of skin subjected to instantaneous heating,'' *IEEE Trans. Biomed. Eng.*, vol. 46, no. 4, pp. 420–428, Apr. 1999.
[9] Z.-S. Deng and J. Liu, ''Analytical study on bioheat transfer problems with spatial or transient heating on skin surface or inside biological bodies,'' *J. Biomechanical Eng.*, vol. 124, no. 6, pp. 638–649, Dec. 2002.
[10] M. Jaunich, S. Raje, K. Kim, K. Mitra, and Z. Guo, ''Bio-heat transfer analysis during short pulse laser irradiation of tissues,'' *Int. J. Heat Mass Transfer*, vol. 51, nos. 23–24, pp. 5511–5521, Nov. 2008.
[11] H. Ahmadikia, A. Moradi, R. Fazlali, and A. B. Parsa, ''Analytical solution of non-Fourier and Fourier bioheat transfer analysis during laser irradiation of skin tissue,'' *J. Mech. Sci. Technol.*, vol. 26, no. 6, pp. 1937–1947, Jun. 2012.
[12] S. Özen, S. Helhel, and O. Çerezci, ''Heat analysis of biological tissue exposed to microwave by using thermal wave model of bio-heat transfer (TWMBT),'' *Burns*, vol. 34, no. 1, pp. 45–49, Feb. 2008.
[13] M. Zhang, Z. Zhou, S. Wu, L. Lin, H. Gao, and Y. Feng, ''Simulation of temperature field for temperature-controlled radio frequency ablation using a hyperbolic bioheat equation and temperature-varied voltage calibration: A liver-mimicking phantom study,'' *Phys. Med. Biol.*, vol. 60, no. 24, pp. 9455–9471, Dec. 2015.
[14] X.-Z. Liu, Y. Zhu, F. Zhang, and X.-F. Gong, ''Estimation of temperature elevation generated by ultrasonic irradiation in biological tissues using the thermal wave method,'' *Chin. Phys. B*, vol. 22, no. 2, Feb. 2013, Art. no. 024301.
[15] Q. Tan, X. Zou, H. Dong, Y. Ding, and X. Zhao, ''Influence of blood vessels on temperature during high-intensity focused ultrasound hyperthermia based on the thermal wave model of bioheat transfer,'' *Adv. Condens. Matter Phys.*, vol. 2018, pp. 1–10, Sep. 2018.
[16] P. Gupta and A. Srivastava, ''Non-Fourier transient thermal analysis of biological tissue phantoms subjected to high intensity focused ultrasound,'' *Int. J. Heat Mass Transf.*, vol. 136, pp. 1052–1063, Jun. 2019.
[17] P. Namakshenas and A. Mojra, ''Numerical study of non-Fourier thermal ablation of benign thyroid tumor by focused ultrasound (FU),'' *Biocybernetics Biomed. Eng.*, vol. 39, no. 3, pp. 571–585, Jul. 2019.
[18] D. Y. Tzou, ''A unified field approach for heat conduction from Macro- to micro-scales,'' *J. Heat Transf.*, vol. 117, no. 1, pp. 8–16, Feb. 1995.
[19] D. Y. Tzou, ''Experimental support for the lagging behavior in heat propagation,'' *J. Thermophys. Heat Transf.*, vol. 9, no. 4, pp. 686–693, Oct. 1995.
[20] D. Y. Tzou, ''Lagging behavior in biological systems,'' *J. Heat Transf.*, vol. 134, no. 5, May 2012, Art. no. 051006.
[21] N. Afrin, J. Zhou, Y. Zhang, D. Y. Tzou, and J. K. Chen, ''Numerical simulation of thermal damage to living biological tissues induced by laser irradiation based on a generalized dual phase lag model,'' *Numer. Heat Transf., A, Appl.*, vol. 61, no. 7, pp. 483–501, Apr. 2012.

[22] K.-C. Liu and J.-C. Wang, "Analysis of thermal damage to laser irradiated tissue based on the dual-phase-lag model," *Int. J. Heat Mass Transf.*, vol. 70, pp. 621–628, Mar. 2014.
[23] K.-C. Liu and H.-T. Chen, "Analysis for the dual-phase-lag bio-heat transfer during magnetic hyperthermia treatment," *Int. J. Heat Mass Transf.*, vol. 52, nos. 5–6, pp. 1185–1192, Feb. 2009.
[24] F. Xu, K. A. Seffen, and T. J. Lu, "Non-Fourier analysis of skin biothermomechanics," *Int. J. Heat Mass Transf.*, vol. 51, nos. 9–10, pp. 2237–2259, May 2008.
[25] M. Lin, Q. D. Liu, T. Kim, F. Xu, B. F. Bai, and T. J. Lu, "A new method for characterization of thermal properties of human enamel and dentine: Influence of microstructure," *Infr. Phys. Technol.*, vol. 53, no. 6, pp. 457–463, Nov. 2010.
[26] C. Li, J. Miao, K. Yang, X. Guo, J. Tu, P. Huang, and D. Zhang, "Fourier and non-Fourier bio-heat transfer models to predict ex vivo temperature response to focused ultrasound heating," *J. Appl. Phys.*, vol. 123, no. 17, May 2018, Art. no. 174906.
[27] W. Kaminski, "Hyperbolic heat conduction equation for materials with a nonhomogeneous inner structure," *J. Heat Transf.*, vol. 112, no. 3, pp. 555–560, Aug. 1990.
[28] A. Vedavarz, S. Kumar, and M. K. Moallemi, "Significance of non-Fourier heat waves in conduction," *J. Heat Transf.*, vol. 116, no. 1, pp. 221–224, Feb. 1994.
[29] K. Mitra, S. Kumar, A. Vedevarz, and M. K. Moallemi, "Experimental evidence of hyperbolic heat conduction in processed meat," *J. Heat Transf.*, vol. 117, no. 3, pp. 568–573, Aug. 1995.
[30] W. Roetzel, N. Putra, and S. K. Das, "Experiment and analysis for non-Fourier conduction in materials with non-homogeneous inner structure," *Int. J. Thermal Sci.*, vol. 42, no. 6, pp. 541–552, Jun. 2003.
[31] F. Duck, *Physical Properties of Tissue: A Comprehensive Reference Book*. London, U.K.: Academic, 1990.
[32] E. A. Zabolotskaya and R. V. Khokhlov, "Quasi-plane waves, in the nonlinear acoustics of confined beams," *Sov. Phys. Acoust.*, vol. 15, pp. 35–40, Jan. 1969.
[33] V. Kuznetsov, "Equation of nonlinear acoustics," *Sov. Phys. Acoust.*, vol. 16, no. 4, pp. 467–470, 1971.
[34] S. A. Goss, R. L. Johnston, and F. Dunn, "Comprehensive compilation of empirical ultrasonic properties of mammalian tissues," *J. Acoust. Soc. Amer.*, vol. 64, no. 2, pp. 423–457, Aug. 1978.
[35] W. Shou, X. Huang, S. Duan, R. Xia, Z. Shi, X. Geng, and F. Li, "Acoustic power measurement of high intensity focused ultrasound in medicine based on radiation force," *Ultrasonics*, vol. 44, pp. e17–e20, Dec. 2006.
[36] S. Maruvada, G. R. Harris, B. A. Herman, and R. L. King, "Acoustic power calibration of high-intensity focused ultrasound transducers using a radiation force technique," *J. Acoust. Soc. Amer.*, vol. 121, no. 3, pp. 1434–1439, Mar. 2007.
[37] H. R. Huang, J. B. Ran, Z. B. Xiao, L. P. Ou, X. Li, J. Xu, Q. Wang, Z. B. Wang, and F. Q. Li, "Reasons for different therapeutic effects of high-intensity focused ultrasound ablation on excised uterine fibroids with different signal intensities on T2-weighted MRI: A study of histopathological characteristics," *Int. J. Hyperthermia*, vol. 36, no. 1, pp. 477–484, Jan. 2019.
[38] J. McLaughlan, I. Rivens, T. Leighton, and G. ter Haar, "A study of bubble activity generated in ex vivo tissue by high intensity focused ultrasound," *Ultrasound Med. Biol.*, vol. 36, no. 8, pp. 1327–1344, Aug. 2010.
[39] L. A. Crum and R. A. Roy, "Sonoluminescence," *Science*, vol. 266, no. 5183, pp. 233–234, Oct. 1994.
[40] B. Liu, J. Cai, and X. Huai, "Heat transfer with the growth and collapse of cavitation bubble between two parallel heated walls," *Int. J. Heat Mass Transf.*, vol. 78, pp. 830–838, Nov. 2014.

CHENGHAI LI was born in 1987. He received the M.D. degree in biomedical engineering from Chongqing Medical University, Chongqing, China, in 2015, and the Ph.D. degree in acoustics from Nanjing University, Nanjing, China, in 2018. He is currently a Postdoctoral Researcher with Chongqing Medical University. His current research interests include ultrasound-induced biological effects and biomedical ultrasound.

SIYAO CHEN was born in 1994. She received the B.S. degree in biomedical engineering from Dali University, Yunnan, China, in 2018. She is currently pursuing the M.D. degree with Chongqing Medical University, Chongqing, China. Her main research interests include biomedical ultrasound and mathematical modeling of sound field in tissue.

QI WANG was born in 1985. He received the B.S. degree in clinical medicine from Chongqing Medical University, Chongqing, China, in 2011. He is currently a Laboratory Technician with Chongqing Medical University. His main research interests include high-intensity focused ultrasound and biomedical engineering.

HAO LI was born in 1996. He received the B.S. degree in functional materials from the Chongqing University of Science and Technology, Chongqing, China, in 2019. He is currently pursuing the M.D. degree with Chongqing Medical University, Chongqing. His main research interests include ultrasound and ultrasound-induced biological effects.

SHUAI XIAO was born in 1995. He received the B.S. degree in electronic information engineering from Nanchang University, Jiangxi, China, in 2019. He is currently pursuing the M.D. degree with Chongqing Medical University, Chongqing, China. His main research interests include biomedical ultrasound and mathematical modeling of sound field in tissue.

FAQI LI was born in 1970. He received the M.D. degree in biomechanics and the Ph.D. degree in biomedical engineering from Chongqing University, Chongqing, China, in 1996 and 1999, respectively. He is currently a Professor with Chongqing Medical University, Chongqing. His current research interests include biomedical ultrasound and biomedical engineering.